

# THE PROBABILITY DISTRIBUTION OF BINARY PULSAR COALESCENCE RATE ESTIMATES. II. NEUTRON STAR–WHITE DWARF BINARIES.

CHUNGLEE KIM<sup>1</sup>, VASSILIKI KALOGERA<sup>1</sup>, DUNCAN R. LORIMER<sup>2</sup>, AND  
TIFFANY WHITE<sup>1</sup>

<sup>1</sup> *Northwestern University, Dept. of Physics & Astronomy, 2145 Sheridan Road, Evanston, IL 60208*

<sup>2</sup> *University of Manchester, Jodrell Bank Observatory, Macclesfield, Cheshire, SK11 9DL, UK.*

*c-kim1@northwestern.edu; vicky@northwestern.edu; drl@jb.man.ac.uk;  
tiphane3@hotmail.com*

## ABSTRACT

We consider the statistics of pulsar binaries with white dwarf companions (NS–WD). Using the statistical analysis method developed by Kim et al. (2003) we calculate the Galactic coalescence rate of NS–WD binaries due to gravitational-wave emission. We find that the most likely values for the total Galactic coalescence rate ( $\mathcal{R}_{\text{tot}}$ ) of NS–WD binaries lie in the range 0.2–10 Myr<sup>-1</sup> depending on different assumed pulsar population models. For our reference model, we obtain  $\mathcal{R}_{\text{tot}} = 4.11_{-2.56}^{+5.25}$  Myr<sup>-1</sup> at a 68% statistical confidence level. These rate estimates are not corrected for pulsar beaming and as such they are found to be about a factor of 20 smaller than the Galactic coalescence rate estimates for double neutron star systems. Based on our rate estimates, we calculate the gravitational-wave background due to coalescing NS–WD binaries out to extragalactic distances within the frequency band of the Laser Interferometer Space Antenna. We find the contribution from NS–WD binaries to the gravitational-wave background to be negligible.

*Subject headings:* binaries: close–gravitational waves–stars: neutron–white dwarfs

## 1. INTRODUCTION

The observed properties of double neutron star (DNS) systems along with models of pulsar survey selection effects have been used for many years in order to estimate the coalescence rate of DNS systems due to the emission of gravitational radiation (Narayan, Piran &

Shemi 1991; Phinney 1991; Curran & Lorimer 1995). In Kim, Kalogera, & Lorimer (2003; hereafter paper I), we presented a novel method to calculate the probability distribution of the coalescence rate estimates for pulsar binaries (see also Kalogera et al. (2004)). In paper I, we applied this method to Galactic DNS systems. Having a probability distribution at hand allowed us to calculate the most likely value for the Galactic DNS coalescence rate as well as statistical confidence limits associated with it. These were then used to calculate the expected DNS inspiral detection rate for Laser Interferometer Gravitational-Wave Observatory (Abramovici et al. 1992). In this second paper, we extend our study to NS–WD binaries that are relevant to the future NASA/ESA mission Laser Interferometer Space Antenna (LISA; Bender et al. 1998) .

There are now more than 40 neutron star-white dwarf (NS–WD) binary systems known in the Galactic disk (see e.g. Lorimer (2001) for a review). Here, we consider the subset of NS–WD binaries which will coalesce due to gravitational-wave (GW) emission within a Hubble time. There are currently three such *coalescing* binaries known: PSR J0751+1807 (Lundgren, Zepka, & Cordes 1995), PSR J1757–5322 (Edwards & Bailes 2001), and PSR J1141–6545 (Kaspi et al. 2000; Bailes et al. 2003). We calculate the Galactic coalescence rate of NS–WD binaries based on their observed properties using the method introduced in paper I. The GW frequencies emitted by these systems fall within the  $\sim 0.1–100$  mHz frequency band of the LISA. Using our rate estimates we calculate the GW amplitude due to the NS–WD binaries out to cosmological distances and compare it to the sensitivity curve of LISA (Larson, Hiscock, & Hellings 2000) as well as the Galactic confusion noise estimates from white dwarf binaries (Bender & Hils 1990, 1997; Nelemans, Yungelson, & Portegies Zwart 2001; Schneider et al. 2001).

The organization of the rest of this paper is as follows. In §2, we consider the lifetimes of NS–WD binaries and summarize the techniques we use to calculate their coalescence rate. The results of these calculations are presented in §3. In §4 we use our rate results to calculate the expected GW background produced by NS–WD binaries. Finally, in §5, we discuss the implications of our results.

## 2. COALESCING NS–WD BINARIES

In general, the coalescence rate of a binary system containing an observable radio pulsar is defined by

$$\mathcal{R} = \frac{N_{\text{PSR}}}{\tau_{\text{life}}} \times f_{\text{b}} , \quad (1)$$

where  $N_{\text{PSR}}^1$  is the estimated number of pulsars in our Galaxy with pulse profiles and orbital characteristics similar to those of the known systems,  $f_b$  is a correction factor for pulsar beaming and  $\tau_{\text{life}}$  is the lifetime of the binary system. In the following subsections, we calculate the total lifetime of a pulsar binary and derive the probability density function (PDF) of the Galactic coalescence rate,  $P(\mathcal{R})$ , for NS–WD binaries.

### 2.1. Lifetime of a NS–WD binary

In Table 1, we summarize the observational properties and relevant lifetimes for the 3 pulsar systems considered in this work. We define the lifetime of a coalescing pulsar binary  $\tau_{\text{life}}$  to be the sum of the current age of the observable pulsar and the remaining lifetime of the system. Assuming the pulsar spins down from an initial period  $P_0$  to the currently observed value  $P$  (both in s) due to a non-decaying magnetic dipole radiation torque (see e.g. Manchester & Taylor (1977)), its current “spin-down” age

$$\tau_{\text{sd}} = \frac{P}{2\dot{P}} \left( 1 - \left[ \frac{P_0}{P} \right]^2 \right), \quad (2)$$

where  $\dot{P}$  (in  $\text{ss}^{-1}$ ) is the observed period derivative. For young pulsars like J1141–6545, it is usually assumed that  $P_0 \ll P$  so that  $\tau_{\text{sd}}$  reduces to the familiar characteristic age  $\tau_c = P/(2\dot{P}) \simeq 1.5$  Myr. For the older recycled pulsars, however, Arzoumanian, Cordes, & Wasserman (1999) pointed out that this assumption is usually not appropriate, since the weaker magnetic fields of these objects mean that their present spin periods are only moderately larger than the periods produced during accretion. Adopting the spin-up line from Arzoumanian, Cordes, & Wasserman (1999), we may write

$$P_0 = \left( \frac{\dot{P}}{1.1 \times 10^{-15}} \right)^{3/4} \text{ s}. \quad (3)$$

Using the above two equations we calculate  $\tau_{\text{sd}}$  for the two recycled pulsars J0751+1807 and J1757–5322 to be 6.7 and 4.9 Gyr respectively (see Table 1).

The remaining lifetime of a pulsar binary is defined by the shorter of the merger time of the binary due to the emission of GWs,  $\tau_{\text{mrg}}$ , or the time that the pulsar will reach the “death line”,  $\tau_d$  (Ruderman & Sutherland 1975). For young pulsars like J1141–6545 which have relatively short radio lifetimes,  $\tau_d < \tau_{\text{mrg}}$ . Recycled pulsars, on the other hand, have far

---

<sup>1</sup>This is equivalent to the so-called ‘scale factor’ (Narayan 1987).

smaller spin-down rates than young pulsars so that it is likely that close binaries containing a recycled pulsar will coalesce before the pulsar reaches the death-line ( $\tau_{\text{mrg}} < \tau_{\text{d}}$ ). For circular orbits, the results of Peters (1964) calculations for the merger time of a binary system of two point masses  $m_1$  and  $m_2$  with orbital period  $P_b$  can be written as simply:

$$\tau_{\text{mrg}} = 9.83 \times 10^6 \text{ yr} \left( \frac{P_b}{\text{hr}} \right)^{8/3} \left( \frac{\mu}{M_\odot} \right)^{-1} \left( \frac{m_1 + m_2}{M_\odot} \right)^{-2/3}, \quad (4)$$

where the reduced mass  $\mu = m_1 m_2 / (m_1 + m_2)$ . For the eccentric binary J1141–6545, we use the more detailed calculations of Peters (1964) to calculate  $\tau_{\text{mrg}}$ . Most of observed coalescing NS–WD binaries as well as the DNS systems have  $\tau_{\text{mrg}} \sim 10^{8-9}$  yr.

Our understanding of pulsar emission is rather poor and therefore it is not clear how to calculate an accurate time associated with the termination of pulsar emission and hence  $\tau_{\text{d}}$ . Here we assume the spin-down torque is dominated by magnetic-dipole radiation with no evolution of the magnetic field. The surface magnetic field of a neutron star,  $B_s$ , can be estimated from the current spin period  $P$  (s) and spin-down rate  $\dot{P}$  ( $\text{ss}^{-1}$ ):

$$B_s = 3.2 \times 10^{19} (P \dot{P})^{1/2} \text{ G}. \quad (5)$$

Chen & Ruderman (1993) comprehensively discussed the evolution of a pulsar period based on different magnetic field structures. Their results are consistent with previous studies (Ruderman & Sutherland 1975; van den Heuvel 1987). We adopt their case C (eq. (9) in their paper) according to which the radio emission terminates when the “death-period”

$$P_{\text{d}} = \left( \frac{B_s}{1.4 \times 10^{11} \text{ G}} \right)^{7/13} \text{ s} \quad (6)$$

is reached. Assuming that the surface magnetic field remains constant, we can integrate eq. (5) to calculate the time for the pulsar period to reach  $P_{\text{d}}$ . We find that

$$\tau_{\text{d}} = \left( \frac{P_{\text{d}}^2 - P^2}{2P\dot{P}} \right). \quad (7)$$

For PSR J1141–6545, we use eqs. (6) and (7) to find the remaining observable lifetime  $\tau_{\text{d}} \sim 104$  Myr. This is significantly less than  $\tau_{\text{mrg}}$  for this binary system ( $\sim 600$  Myr). Including the modest contribution from the characteristic age of J1141–6545, we take the observable lifetime of the binary system to be  $\tau_{\text{life}} = \tau_{\text{c}} + \tau_{\text{d}} \sim 105$  Myr. We note in passing that Edwards & Bailes (2001) estimated the remaining lifetime of PSR J1141–6545 to be only  $\sim 10$  Myr. Although no details of their calculation were presented in their paper, they probably assumed some decay of the magnetic field which led to their lower value  $\tau_{\text{d}}$  and hence  $\tau_{\text{life}}$ .

In the cases of the recycled pulsars J0751+1807 and J1757–5322, which have lower magnetic field strengths and hence longer radio lifetimes, both binaries will coalesce before the pulsars stop radiating (i.e.  $\tau_{\text{mrg}} \ll \tau_{\text{d}}$ ), so we calculate their lifetime using  $\tau_{\text{life}} = \tau_{\text{sd}} + \tau_{\text{mrg}}$ . The estimated lifetimes are 14.3 Gyr (J0751+1807) and 12.7 Gyr (J1757–5322), about two orders of magnitude longer than for the young NS–WD J1141–6545.

## 2.2. Probability Density Function of the Galactic NS–WD Coalescence Rate Estimates

The basic strategy we use to calculate  $P(\mathcal{R}_{\text{tot}})$  is described in detail in paper I. In brief, using a detailed Monte Carlo simulation, for each observed NS–WD binary, we determine the fraction of the population that is actually *detectable* by careful modeling of all large-scale pulsar surveys. We include the selection effects that reduce the detectability of short-period binary systems when integration times are significant in comparison. Our pulsar population model takes into account the distribution of pulsars in the Galaxy and their luminosity function. Treating each pulsar separately, our simulations effectively probe the specific pulsar sub-populations with pulse and orbital characteristics similar to those of PSR J0751+1807, J1757–5322, or J1141–6545.

From the simulations we obtain  $N_{\text{obs}}$  pulsars detected by the surveys out of a Galactic population of  $N_{\text{tot}}$  in each model. We calculate  $N_{\text{obs}}$  repeatedly for a fixed  $N_{\text{tot}}$ . As shown in detail in paper I, the distribution of  $N_{\text{obs}}$  follows a Poisson function,  $P(N_{\text{obs}}; \langle N_{\text{obs}} \rangle)$ . We calculate the best-fit value of  $\langle N_{\text{obs}} \rangle$ , which is the mean number of observed pulsars in a given sample, for a given  $N_{\text{tot}}$ . Since we consider each observed pulsar separately, we set  $N_{\text{obs}} = 1$ . For example, one PSR J0751+1807 and no other pulsar similar to this (in terms of spin and orbital properties of the pulsar) have been observed. The likelihood of detecting *one pulsar* similar to the observed one from the given pulsar population with  $N_{\text{tot}}$  samples is simply  $P(1; \langle N_{\text{obs}} \rangle)$ . We vary  $N_{\text{tot}}$  and calculate  $P(1; \langle N_{\text{obs}} \rangle)$  to determine the most probable value of  $N_{\text{tot}}$ . Also, we found  $\langle N_{\text{obs}} \rangle$  is directly proportional to  $N_{\text{tot}}$ . We calculate  $\alpha$ , which is the slope of the function  $\langle N_{\text{obs}} \rangle = \alpha N_{\text{tot}}$  for each observed system for a pulsar population model.

Then, using Bayes’ theorem, we calculate  $P(\langle N_{\text{obs}} \rangle)$  from the likelihood  $P(1; \langle N_{\text{obs}} \rangle)$  and eventually calculate  $P(\mathcal{R})$  using a change of variables. We repeat the whole procedure for all three observed coalescing NS–WD binaries, and combine the three individual PDFs to obtain a total PDF of Galactic coalescence rate of NS–WD binaries,  $P(\mathcal{R}_{\text{tot}})$ .

In paper I, we showed that a normalized PDF of the coalescence rate for an individual

pulsar binary system can be written as follows:

$$P_i(\mathcal{R}) = C_i^2 \mathcal{R} e^{-C_i \mathcal{R}}, \quad (8)$$

where  $C_i$  is a coefficient determined by properties of the  $i^{\text{th}}$  pulsar:

$$C_i \equiv \left( \frac{\alpha \tau_{\text{life}}}{f_b} \right)_i. \quad (9)$$

Here, the beaming correction factor  $f_b$  is the inverse of the fraction of  $4\pi$  sr covered by the pulsar radiation beam during each rotation. In the case of the two DNS systems, PSRs B1913+16 and B1534+12, Kalogera et al. (2001) adopted  $f_b \sim 6$  based on pulse profile and polarization measurements of two pulsars. The lack of such observations for the current sample of NS–WD binaries means that it is difficult to estimate reliable values of  $f_b$ . Therefore, in this paper, we do not correct for pulsar beaming (i.e.  $f_b = 1$ ). As a result, all our values should be considered as lower limits.

In paper I, we calculated  $P(\mathcal{R}_{\text{tot}})$  considering two observed DNSs systems (labeled by the subscripts 1 and 2). We defined the total rate  $\mathcal{R}_+ \equiv \mathcal{R}_1 + \mathcal{R}_2$  and showed that

$$P(\mathcal{R}_+) = \left( \frac{C_1 C_2}{C_2 - C_1} \right)^2 \left[ \mathcal{R}_+ \left( e^{-C_1 \mathcal{R}_+} + e^{-C_2 \mathcal{R}_+} \right) - \left( \frac{2}{C_2 - C_1} \right) \left( e^{-C_1 \mathcal{R}_+} - e^{-C_2 \mathcal{R}_+} \right) \right], \quad (10)$$

where  $C_1 < C_2$ . In Appendix A, we show that this can be extended for the current case of interest where we have three binary systems such that  $\mathcal{R}_+ \equiv \mathcal{R}_1 + \mathcal{R}_2 + \mathcal{R}_3$ . This leads to

$$\begin{aligned} P(\mathcal{R}_+) = & \frac{C_1^2 C_2^2 C_3^2}{(C_2 - C_1)^3 (C_3 - C_1)^3 (C_3 - C_2)^3} \left[ \right. \quad (11) \\ & (C_3 - C_2)^3 e^{-C_1 \mathcal{R}_+} \left[ -2(-2C_1 + C_2 + C_3) + \mathcal{R}_+ [-C_1(C_2 + C_3) + (C_1^2 + C_2 C_3)] \right] \\ & + (C_3 - C_1)^3 e^{-C_2 \mathcal{R}_+} \left[ 2(C_1 - 2C_2 + C_3) + \mathcal{R}_+ [C_2(C_3 + C_1) - (C_2^2 + C_3 C_1)] \right] \\ & \left. + (C_2 - C_1)^3 e^{-C_3 \mathcal{R}_+} \left[ -2(C_1 + C_2 - 2C_3) + \mathcal{R}_+ [-C_3(C_1 + C_2) + (C_3^2 + C_1 C_2)] \right] \right], \end{aligned}$$

where the coefficients  $C_i$  ( $i = 1, 2, 3$ ) are defined by eq. (9) and  $C_1 < C_2 < C_3$ . This result was already used in our recent rate estimation for DNS systems to include the newly discovered pulsar, J0737-3039 (Burgay et al. 2003; Kalogera et al. 2004). As before, the confidence limit (CL)<sup>2</sup> and the lower and upper limits ( $\mathcal{R}_L$  and  $\mathcal{R}_U$ ) of the coalescence rate estimates are

---

<sup>2</sup>Strictly speaking, the phrase “confidence limit” used in this paper should be interpreted as a confidence *interval* such that a true value of the Galactic coalescence rate would exist in a given range of rates. However, we keep the terminology *confidence limit* for consistency with paper I and Kalogera et al. (2004).

defined in the same way we described in paper I, i.e.

$$\int_{\mathcal{R}_L}^{\mathcal{R}_U} P(\mathcal{R}_+) d\mathcal{R}_+ = \text{CL} , \quad (12)$$

and

$$P(\mathcal{R}_L) = P(\mathcal{R}_U) . \quad (13)$$

### 3. RESULTS

In Fig. 1, we show the resulting  $P(\mathcal{R}_{\text{tot}})$  for NS–WD binaries along with the individual PDFs for each observed coalescing binaries. The figure shown here is obtained from our reference model (model 6 in paper I). As we found for the DNS systems in paper I,  $P(\mathcal{R}_{\text{tot}})$  is highly peaked and dominated by a single object. In this case, PSR J1141–6545 dominates the results by virtue of its short observable lifetime ( $\tau_{\text{life}} \sim 105$  Myr). This is in spite of the fact that the estimated total number of binaries similar to PSR J0751+1807 ( $N_{0751} \simeq 2900$ ) is the largest among the observed systems.

We summarize our results for different pulsar population models in Table 2. The model parameters are identical to those described in paper I. We note however, following Kalogera et al. (2004), that our reference model is now model 6 ( $L_{\text{min}} = 0.3$  mJy kpc<sup>2</sup>) rather than model 1 ( $L_{\text{min}} = 1.0$  mJy kpc<sup>2</sup>). This choice reflects the recent discoveries of faint pulsar with 1400-MHz radio luminosities below than 1.0 mJy kpc<sup>2</sup> (Camilo 2003). The peak values of  $P(\mathcal{R}_{\text{tot}})$  lie in the range between  $\sim 0.2 - 10$  Myr<sup>-1</sup> where the reference model shows a peak around 4 Myr<sup>-1</sup>. For the reference model, the uncertainties in the rates, (defined by  $\mathcal{R}_U/\mathcal{R}_L$ ) are estimated to be  $\sim 6, 27$  and  $62$  at 68%, 95%, and 99% CL, respectively. Comparing this to results from Kalogera et al. (2004), we find that the uncertainties at different CL of the coalescence rate of NS–WD binaries are typically larger by factor of  $\sim 1.4$  than those of the DNS systems. This result is robust for all models we consider.

The correlations between the peak value of the total Galactic coalescence rate  $\mathcal{R}_{\text{peak}}$  and the model parameters (e.g. the cut-off luminosity  $L_{\text{min}}$  and the power index  $p$ ) seem to be similar to those of DNSs we observed in paper I. As we found for the DNS systems,  $\mathcal{R}_{\text{peak}}$  values strongly depend on a pulsar luminosity function rather than a spatial distribution of pulsars in the Galaxy, in other words,  $\mathcal{R}_{\text{peak}}$  values rapidly increase as the fraction of faint pulsars increases.

#### 4. GRAVITATIONAL WAVE BACKGROUND DUE TO NS–WD BINARIES

Close binaries consisting of compact objects (e.g. NS–WD binaries) are suggested as important GW sources in a frequency range below 1 mHz. In this range, due to the large number of sources, LISA would not be able to resolve each source within a given frequency band. Hence the Galactic binaries are expected to establish a confusion noise level (or “background”) dominated by WD–WD binaries (Bender & Hils 1990, 1997; Nelemans, Yungelson, & Portegies Zwart 2001; Schneider et al. 2001). In this work, we consider the contribution from NS–WD binaries to the predicted confusion noise level. Using our results from the previous section, we calculate the amplitude of GW signals from NS–WD binaries in the nearby Universe and compare it with the LISA sensitivity curve<sup>3</sup>. In this work, we assume that the three observed systems represent the whole population of NS–WD binaries in our Galaxy.

We calculate the characteristic strain amplitude of GWs ( $h_c$ ) from NS–WD binaries using the results given by Phinney (2001) for circular binaries. In general, binaries with an eccentricity  $e$  emit GWs at frequencies  $f = n\nu$ , i.e. the  $n$ -th harmonic of the orbital frequency  $\nu$ . In the case of circular binaries,  $n = 2$  due to the orbital symmetry and the quadrupole nature of GWs. The eccentricity of PSRs J0751+1807 and J1757–5322 are  $e \sim 10^{-4}$  and  $\sim 10^{-6}$ , respectively. Hence, it is safe to consider them as circular binaries. PSR J1141–6545 has an appreciable eccentricity ( $e = 0.17$ ), but for simplicity, we consider only the  $n = 2$  harmonic as if it were a circular binary<sup>4</sup>.

For an observation of length  $T_{\text{obs}}$  with a GW detector, the contribution from background sources (NS–WD binaries in this work) depends on the number of sources within the frequency resolution,  $\Delta f = 1/T_{\text{obs}}$ . Following Schneider et al. (2001), we define an effective GW amplitude  $h_{\text{rms}}(f) \equiv h_c(f)(\Delta f/f)^{1/2}$ , where  $h_c(f)$  is a characteristic strain amplitude. Phinney (2001) showed a simple analytic formula to calculate  $h_c(f)$  for a population of inspiraling circular-orbit binaries with a given number density in the nearby Universe. We

---

<sup>3</sup>We use the online sensitivity curve generator to calculate the sensitivity curve of LISA (<http://www.srl.caltech.edu/shane/sensitivity/MakeCurve.html>).

<sup>4</sup>We calculate the power distribution in various harmonics for this eccentricity based on the result of Peters & Mathews (1963). We note that the GW amplitude calculated for J1141–6545 in this work corresponds to  $\sim 70\%$  of the total power of the gravitational radiation emitted from this binary. The remaining power is contributed from the higher harmonics.



use eq. (16) in his paper to calculate  $h_c(f)^5$ , and find

$$h_{\text{rms}}(f) \simeq 1.7 \times 10^{-26} \left( \frac{\mathcal{M}}{M_\odot} \right)^{5/6} \left( \frac{f}{\text{mHz}} \right)^{-7/6} \left( \frac{N_o}{\text{Mpc}^{-3}} \right)^{1/2} \left( \frac{T_{\text{obs}}}{\text{yr}} \right)^{-1/2}, \quad (14)$$

where  $\mathcal{M}$  is the “chirp mass” of a NS–WD binary defined by

$$\mathcal{M} \equiv \frac{(M_{\text{NS}} M_{\text{WD}})^{3/5}}{(M_{\text{NS}} + M_{\text{WD}})^{1/5}}, \quad (15)$$

and  $N_o$  is the comoving number density of NS–WD, i.e. the number of sources per  $\text{Mpc}^3$ .

We calculate the GW amplitude of NS–WD binaries in a frequency range  $f_{\text{min}} < f < f_{\text{max}}$ . Estimated GW frequencies of three NS–WD binaries based on their current separations are all less than  $\sim 0.1$  mHz. In our calculation, however, we set the minimum frequency  $f_{\text{min}}$  to be 1 mHz taking into account the fact that the confusion noise level is mainly dominated by Galactic WD–WD binaries at lower frequency range  $f < 1$  mHz (Nelemans, Yungelson, & Portegies Zwart 2001). The maximum GW frequency  $f_{\text{max}}$  is calculated by  $f_{\text{max}} = 2/P_{\text{b,min}}$ , where  $P_{\text{b,min}}$  is the minimum orbital period of the binary at the WD Roche-lobe overflow.

Following Eggleton (1983), we calculate the minimum possible separation of the binary using  $a_{\text{min}} = R_{\text{WD}}/r_{\text{L}}$ , where  $r_{\text{L}}$  is the effective Roche lobe radius. We estimate the radius of a white dwarf companion  $R_{\text{WD}}$  adopting the results given by Tout, Aarseth, & Pols (1997). We show the estimated mass of white dwarf companions in Table 1. Converting  $a_{\text{min}}$  to  $f_{\text{max}}$  based on the Kepler’s 3rd law, we find that

$$f_{\text{max}} \simeq 0.16 r_{\text{L}}^{3/2} \left( \frac{M_{\text{WD}} + M_{\text{NS}}}{M_\odot} \right)^{1/2} \left[ \left( \frac{M_{\text{ch}}}{M_{\text{WD}}} \right)^{2/3} - \left( \frac{M_{\text{WD}}}{M_{\text{ch}}} \right)^{2/3} \right]^{-3/4} \text{ Hz}, \quad (16)$$

where  $M_{\text{ch}} = 1.44M_\odot$  is the Chandrasekhar limit. We note that  $f_{\text{max}} = f_{\text{max}}(M_{\text{NS}}, M_{\text{WD}})$ . Based on eq. (16), we define three frequency regions: (a)  $f_{\text{min}} < f < f_{\text{max}, 0751}$ , (b)  $f_{\text{max}, 0751} < f < f_{\text{max}, 1757}$ , and (c)  $f_{\text{max}, 1757} < f < f_{\text{max}, 1141}$ . In the region (a), for example, all three observed NS–WD systems contribute to the GW background. However, for frequencies larger than  $f_{\text{max}, 0751}$ , PSR J0751+1807-like populations have already reached the Roche lobe overflow and we can not apply eq. (14) to these systems. Therefore, in a frequency region (b), we consider J1141–6545-like and J1757–5322-like populations. Similarly, for the highest frequency range (region (c)), we consider the contribution to the GW signals from PSR J1141–6545-like population only.

---

<sup>5</sup>We assume a case that the last term in Phinney’s eq. (16),  $\left( \frac{\langle (1+z)^{-1/3} \rangle}{0.74} \right)^{1/2}$  becomes unity. The calculation is not significantly affected by different assumptions on cosmological models and comoving number density functions of coalescing binaries (Phinney (2001)).

In order to calculate  $h_{\text{rms}}(f)$ , we need the chirp mass  $\mathcal{M}$  and present-day comoving number density of NS–WD binaries  $N_o$ . Following Farmer & Phinney (2002), we define the “flux-weighted” averaged chirp mass:

$$\langle \mathcal{M} \rangle \equiv \frac{\sum \mathcal{F}_{\text{gw},i} \mathcal{M}_i}{\sum \mathcal{F}_{\text{gw},i}} = \frac{\sum \mathcal{N}_{\text{peak},i} \mathcal{M}_i^{13/3}}{\sum \mathcal{N}_{\text{peak},i} \mathcal{M}_i^{10/3}}, \quad (17)$$

where  $\mathcal{F}_{\text{gw}}$  is the GW flux ( $\mathcal{F}_{\text{gw}} \propto f^{10/3} \mathcal{M}^{10/3} \mathcal{N}_{\text{peak}}$ ) and  $\mathcal{N}_{\text{peak}}$  is the peak value of  $P(N_{\text{tot}})$  of the each sub-population of NS–WD binaries in our Galaxy. The subscript  $i$  represents each pulsar sub-population. For example, in region (b),  $\langle \mathcal{M} \rangle = (\mathcal{N}_{1757} \mathcal{M}_{1757}^{13/3} + \mathcal{N}_{1141} \mathcal{M}_{1141}^{13/3}) / (\mathcal{N}_{1757} \mathcal{M}_{1757}^{10/3} + \mathcal{N}_{1141} \mathcal{M}_{1141}^{10/3})$ . Because  $\mathcal{N}_{\text{peak}}$  is a constant and independent of the GW frequency, it follows that  $\langle \mathcal{M} \rangle$  is independent of frequency. As a result, the evolution of orbital characteristics and hence the GW frequency of a binary are solely determined by the inspiral process. This is true regardless of the initial distribution of orbital characteristics.

We now calculate the comoving number density of NS–WD binaries

$$N_o = \int_0^\infty N(z) dz, \quad (18)$$

where  $N(z)dz$  is the number of NS–WD binaries per unit comoving volume between redshift  $z$  and  $z + dz$ . Noting that the number density of NS–WD binaries is proportional to the total number of systems, we may write

$$N_o = \epsilon \mathcal{N}_{\text{PSR}}, \quad (19)$$

where  $\epsilon$  is the star formation rate density per unit comoving volume ( $\dot{\rho}$ ) normalized to the Galactic star formation rate ( $r$ ) i.e.  $\epsilon = \dot{\rho}/r$  (in  $\text{Mpc}^{-3}$ ).  $\mathcal{N}_{\text{PSR}}$  is the most likely value of the total number of pulsars for each frequency range. (e.g.  $\mathcal{N}_{\text{PSR}} = \mathcal{N}_{0751} + \mathcal{N}_{1757} + \mathcal{N}_{1141}$  in region (a)). We derived  $P(N_{\text{tot}})$  for individual systems in paper I. In a similar fashion to the coalescence rate estimation described in Appendix A, the combined PDF of  $N_{\text{tot}}$  can be calculated from individual PDFs of the observed systems. Then  $\mathcal{N}_{\text{PSR}}$  can be obtained from the peak value of the PDF we calculate for each frequency range we discussed above.

Using the results of Cole et al. (2001), we find

$$\epsilon = \frac{\dot{\rho}(0)}{r} \int_0^{z_{\text{max}}} \frac{(1 + \frac{b}{a}z)}{(1 + (\frac{z}{c})^d)} dz \quad \text{Mpc}^{-3}, \quad (20)$$

where  $(a, b, c, d) = (0.0166, 0.1848, 1.9474, 2.6316)$  are parameters which take into account dust-extinction corrections (see Cole et al. (2001) for further details). Assuming a Hubble

constant  $H_0 = 65 \text{ km s}^{-1} \text{ Mpc}^{-1}$ , we calculate the Galactic star formation rate density  $\dot{\rho}(0) \simeq 0.01 \text{ M}_\odot \text{ yr}^{-1} \text{ Mpc}^{-3}$ . Following Cappellaro, Evans, & Turatto (1999), assuming the Salpeter initial mass function, we convert the Galactic supernova type  $\text{SN}_{\text{II+Ib/c}}$  rate<sup>6</sup> to the star formation rate finding  $r \sim 0.7 \text{ M}_\odot \text{ yr}^{-1}$ . Numerically integrating eq. (20) out to  $z_{\text{max}} = 5$ , which is considered to be the onset of the galaxy formation (Schneider et al. 2001), we find  $\epsilon \sim 0.6 \text{ Mpc}^{-3}$ . The number density of NS–WD binaries  $N_0$  then can be calculated by eq. (19) for a given  $\mathcal{N}_{\text{PSR}}$  for each model.

In Fig. 2, we plot the GW amplitude  $h_{\text{rms}}$  against the simulated LISA sensitivity curve calculated for a signal-to-noise ratio  $S/N=1$ . All dotted lines correspond to the GW amplitude calculated from the full set of pulsar population models we consider and the solid line is the result from our reference model. The range of the GW amplitude for all models spans about an order of magnitude. We find that the GW background amplitude from NS–WD binaries is about 1–2 orders of magnitude smaller than the expected sensitivity curve of LISA at GW frequencies larger than 1mHz and it is unlikely that this population will be detected with LISA. In the lower frequency region (below  $\sim 1\text{mHz}$ ), the GW background amplitude from NS–WD binaries increases as  $f$  decreases. However, the contribution from NS–WD binaries to the GW background noise level would still be less than  $\sim 10\%$  of the GW amplitude from WD–WD binaries (dashed line in 2). We note that, however, we have not considered any beaming corrections, so the NS–WD background curves should be viewed as lower limits. This possibility is discussed briefly in the next section.

## 5. DISCUSSION

We have used detailed Monte Carlo simulations to calculate the Galactic coalescence rate of NS–WD binaries. From the reference model, the most probable value of  $\mathcal{R}_{\text{tot}}$  is estimated to be  $4.11_{-2.56}^{+5.25} \text{ Myr}^{-1}$  at a 68% statistical confidence limit. We find that the coalescence rate of NS–WD binaries is about factor of 20 smaller than those of DNS for all pulsar population models we consider. As mentioned above, we did not take into account any beaming correction for NS–WD binaries. If we assume a beaming fraction of pulsars in NS–WD binaries similar to that of pulsars found in DNS,  $f_b \sim 6$ , then the discrepancy between  $\mathcal{R}_{\text{peak}}$  (DNS) and  $\mathcal{R}_{\text{peak}}$  (NS–WD) is significantly reduced. As a simple estimate, if we assume  $f_{b,1141} \sim 5$ , but keeping  $f_b = 1$  for the other two binaries, the estimated

---

<sup>6</sup>Cappellaro, Evans, & Turatto (1999) assumed a Hubble constant  $H_0 = 75 \text{ km s}^{-1} \text{ Mpc}^{-1}$ . Since we adopt  $H_0 = 65 \text{ km s}^{-1} \text{ Mpc}^{-1}$ , we have multiplied their results by a factor  $(65/75)^2$ . We also note that we consider Sbc-Sd type galaxies only, which would be relevant for active star-forming regions.

Galactic coalescence rate increases to  $18.06_{-12.74}^{+26.05}$  Myr<sup>-1</sup> at a 68% confidence limit. Hence the ratio between DNS and NS–WD coalescence rate decreases to about 5. Because the contribution from PSRs J0751+1807 and J1757–5322 is an order of magnitude smaller than that of J1141–6545, moderate values of beaming fraction for those recycled pulsars do not change the result significantly.

Based on the number of sources of NS–WD binaries in our Galaxy, we estimate the effective GW amplitude from the cosmic population of these systems. We find that the GW background from NS–WD binaries is too weak to be detected by LISA for the nominal beaming correction. Only by adopting an unreasonably large beaming correction factor,  $f_b > 10$ , could these systems be detectable by LISA in the mHz range. These results are in good agreement with an independent study by Cooray (2004) based on statistics of low mass X-ray binaries.

We finally note that combining the results from paper I and this work can give us strong constraints on the population synthesis models. The preferred models, which are consistent with both  $\mathcal{R}_{\text{NS–WD}}$  and  $\mathcal{R}_{\text{DNS}}$ , can then be used for the estimation of the coalescence rate of neutron star – black hole binaries, which have not yet been observed.

We thank A. Cooray for noticing the frequency resolution correction factor in the calculation of the GW background. This work is partially supported by NSF grant PHY-0121420 and a Packard Fellowship in Science and Engineering to VK. DRL is a University Research Fellow funded by the Royal Society. He is also grateful for support from the Theoretical Astrophysics Visitors’ Fund at Northwestern University.

## REFERENCES

- Abramovici et al. 1992, *Science*, 256, 325
- Arzoumanian, Z. , Cordes, J. M. , & Wasserman, I. 1999, *ApJ*, 520, 696
- Bailes, M. , Ord, S. M. , Knight, H. S. , & Hotan, A. W. 2003, *ApJ*, 595, L49
- Bender, P. et al. 1998, *LISA Pre-Phase A Report*, 2nd ed.
- Hils, D. , & Bender, P. L. 1990 *ApJ*, 360, 75
- Bender, P. L. , & Hils, D. 1999 *Class. Quantum Grav.*, 14, 1439
- Burgay, M. et al. 2003, *Nature* 426, 531

- Camilo, F. 2003, ASP Conf. Ser. *Radio Pulsars*, ed. Bailes, M., Nice, D. J., & Thorsett, S. E. (San Francisco: ASP) **302**, 145
- Cappellaro, E., Evans, R., & Turatto, M. 1999, *A&A*, 351, 459
- Chen, K., & Ruderman, M. 1993, *ApJ*, 402, 264
- Cole, S. et al. 2001, *MNRAS*, 326, 255
- Curran, S. J. & Lorimer, D. R. 1995, *MNRAS*, 276, 347
- Cooray, A. 2004, *MNRAS*, in press
- Edwards, R. T. & Bailes, M. 2001, *ApJ*, 547, L37
- Eggleton, P. P. 1983, *ApJ*, 268, 368
- Farmer, A. J. & Phinney, E. S. 2002, astro-ph/0304393
- Kalogera, V., Narayan, R., Spergel, D. N., & Taylor J. H. 2001, *ApJ*, 556, 340 (KNST)
- Kalogera et al. 2004, *ApJ*, in press
- Kaspi, V. M., Lyne, A. G., Manchester, R. N., Crawford, F., Camilo, F., Bell, J. F., D’Amico, N. D., Stairs, I. H., McKay, N. P. F., Morris, D. J., & Possenti, A. 2000, *ApJ*, 543, 321
- Kim, C., Kalogera, V., & Lorimer, D. 2003, *ApJ*, 584, 985 (paper I)
- Larson, S. L., Hiscock W. A., & Hellings, R. W. 2000, *Phys. Rev. D*, 62, 062001
- Lorimer, D. R., 2001, *Living Rev. in Relativity*, 4, 5 (online)  
<http://www.livingreviews.org/Articles/Volume4/2001-5lorimer/>
- Lundgren, S. C., Zepka, A. F., & Cordes, J. M. 1995, *ApJ*, 453, 419
- Manchester, R. N., & Taylor, J. H. 1977, *Pulsars*, Freeman, San Fransico
- Narayan, R. 1987, *ApJ*, 319, 162
- Narayan, R., Piran, T., & Shemi, A. 1991, *ApJ*, 379, L17
- Nelemans, G., Yungelson, L. R., & Portegies Zwart, S. F. 2001, *A&A*, 375, 890
- Nice, D. J., Splaver, E. M., & Stairs, I. H. 2004, *IAU 218*, 49

Peters, P. C. 1964, Phys. Rev. 136, B1224

Peters, P. C. & Mathews, J. 1963, Phys. Rev. D, 131, 435

Phinney, E. S. 1991, ApJ, 380, L17

Phinney, E. S. astro-ph/0108028

Ruderman, M. A. & Sutherland, P. G. 1975, ApJ, 196, 51

Schneider, R. , Ferrari, V. , Matarrese, S. , & Portegies Zwart, S. F. 2001, MNRAS, 324, 797

Tout, C. A. , Aarseth, S. J. , & Pols, O. R. 1997, MNRAS, 291, 732

van den Heuvel, E. P. J. 1987, IAUS, 125, 393

van Kerkwijk, M. H. & Kulkarni, S. R. 1999, ApJ, 516, L25

### A. Combined rate PDF for three binary systems

In paper I, we derived expressions for  $P(\mathcal{R}_{\text{tot}})$  for one and two coalescing binaries. In this paper, and in our revised DNS coalescence rate estimates (Kalogera et al. 2004), we extend this PDF to the case of three systems. Following paper I, we define a coefficient for each observed NS–WD:

$$A \equiv \left( \frac{\alpha \tau_{\text{life}}}{f_{\text{b}}} \right)_{1141}, B \equiv \left( \frac{\alpha \tau_{\text{life}}}{f_{\text{b}}} \right)_{0751}, \text{ and } C \equiv \left( \frac{\alpha \tau_{\text{life}}}{f_{\text{b}}} \right)_{1757}, \quad (\text{A1})$$

where  $A < B < C$ . Recall that  $\alpha$  is the slope of the function  $\langle N_{\text{obs}} \rangle = \alpha N_{\text{tot}}$  and is determined for each pulsar population model for each NS–WD system. By definition, the total Galactic coalescence rate is the sum of all three observed systems:

$$\mathcal{R}_{+} \equiv \mathcal{R}_1 + \mathcal{R}_2 + \mathcal{R}_3. \quad (\text{A2})$$

Redefining  $\mathcal{R}_{+} \equiv \mathcal{R}_a + \mathcal{R}_b$ , where  $\mathcal{R}_a \equiv \mathcal{R}_1 + \mathcal{R}_2$  and  $\mathcal{R}_b \equiv \mathcal{R}_3$ , we transform  $\mathcal{R}_a$  and  $\mathcal{R}_b$  to new variables  $\mathcal{R}_{+}$  and  $\mathcal{R}_{-} \equiv \mathcal{R}_a - \mathcal{R}_b$

$$P(\mathcal{R}_{+}, \mathcal{R}_{-}) = P(\mathcal{R}_a, \mathcal{R}_b) \left| \begin{array}{cc} \frac{d\mathcal{R}_a}{d\mathcal{R}_{+}} & \frac{d\mathcal{R}_b}{d\mathcal{R}_{-}} \\ \frac{d\mathcal{R}_a}{d\mathcal{R}_{-}} & \frac{d\mathcal{R}_b}{d\mathcal{R}_{+}} \end{array} \right| = \frac{1}{2} P(\mathcal{R}_a, \mathcal{R}_b). \quad (\text{A3})$$

Since both  $\mathcal{R}_+$  and  $\mathcal{R}_-$  are positive,  $-\mathcal{R}_- \leq \mathcal{R}_+ \leq +\mathcal{R}_-$ .

The PDF of the total rate  $\mathcal{R}_+$  is obtained after integrating  $P(\mathcal{R}_+, \mathcal{R}_-)$  over  $\mathcal{R}_-$ :

$$P(\mathcal{R}_+) = \int_{\mathcal{R}_-} P(\mathcal{R}_+, \mathcal{R}_-) d\mathcal{R}_- = \frac{1}{2} \int_{\mathcal{R}_-} P(\mathcal{R}_a, \mathcal{R}_b) d\mathcal{R}_-, \quad (\text{A4})$$

where

$$P(\mathcal{R}_a, \mathcal{R}_b) = P(\mathcal{R}_a)P(\mathcal{R}_b). \quad (\text{A5})$$

Here,  $P(\mathcal{R}_a = \mathcal{R}_1 + \mathcal{R}_2)$  is given by eq. (10) and we can rewrite the formula with appropriate coefficients defined earlier:

$$P(\mathcal{R}_a) = \left(\frac{AB}{B-A}\right)^2 \left[ \mathcal{R}_a \left( e^{-A\mathcal{R}_a} + e^{-B\mathcal{R}_a} \right) - \left(\frac{2}{B-A}\right) \left( e^{-A\mathcal{R}_a} - e^{-B\mathcal{R}_a} \right) \right]. \quad (\text{A6})$$

The individual PDF  $P(\mathcal{R}_b) \equiv P(\mathcal{R}_3)$  (eq. (8)) is also rewritten as follows:

$$P_i(\mathcal{R}_b) = C^2 \mathcal{R}_b e^{-C\mathcal{R}_b}. \quad (\text{A7})$$

Replacing  $\mathcal{R}_a = (1/2)(\mathcal{R}_+ + \mathcal{R}_-)$  and  $\mathcal{R}_b = (1/2)(\mathcal{R}_+ - \mathcal{R}_-)$  in eq. (A4), the normalized  $P(\mathcal{R}_+)$  can be obtained by integration. After some algebra, we find:

$$\begin{aligned} P(\mathcal{R}_+) &= \frac{A^2 B^2 C^2}{(B-A)^3 (C-A)^3 (C-B)^3} \quad (\text{A8}) \\ &\left[ (C-B)^3 e^{-A\mathcal{R}_+} \left[ -2(-2A+B+C) + \mathcal{R}_+ [-A(B+C) + (A^2+BC)] \right] \right. \\ &+ (C-A)^3 e^{-B\mathcal{R}_+} \left[ 2(A-2B+C) + \mathcal{R}_+ [B(C+A) - (B^2+CA)] \right] \\ &\left. + (B-A)^3 e^{-C\mathcal{R}_+} \left[ -2(A+B-2C) + \mathcal{R}_+ [-C(A+B) + (C^2+AB)] \right] \right]. \end{aligned}$$

Table 1. Observational properties of NS–WD binaries. From left to right, the columns indicate the pulsar name, spin period  $P$ , spin-down rate  $\dot{P}$ , orbital period  $P_b$ , most probable mass of the WD companion  $m_{\text{wd}}$ , orbital eccentricity  $e$ , characteristic age  $\tau_c$ , spin-down age  $\tau_{\text{sd}}$ , GW merger timescale  $\tau_{\text{mrg}}$ , time to reach the death line  $\tau_d$ , most probable number of NS–WD systems of this type in the Galaxy and references to this system in the literature.

PSRs	$P$ (ms)	$\dot{P}$ (s s <sup>-1</sup> )	$P_b$ (hr)	$m_{\text{wd}}^a$ (M <sub>⊙</sub> )	$e$	$\tau_c$ (Gyr)	$\tau_{\text{sd}}$ (Gyr)	$\tau_{\text{mrg}}$ (Gyr)	$\tau_d$ (Gyr)	$\mathcal{N}_{\text{PSR}}$	References <sup>b</sup>
J0751+1807	3.479	$8.08 \times 10^{-21}$	6.315	0.18	$< 10^{-4}$	6.8	6.7	7.6	...	2900	1, 2
J1757–5322	8.870	$2.78 \times 10^{-20}$	10.88	0.67	$10^{-6}$	5.1	4.9	7.8	...	1200	3
J1141–6545	393.9	$4.29 \times 10^{-15}$	4.744	0.986	0.172	$1.5 \times 10^{-3}$	...	0.6	0.104	400	4,5

<sup>a</sup>The assumed NS mass and inclination angle  $i$  are  $2.2M_{\odot}$  and  $78^{\circ}$  for J0751+1807 (Nice et al. (2004)) and  $1.35M_{\odot}$  and  $60^{\circ}$  for J1757–5322. For PSR J1141–6545, we adopt values given in Bailes et al. (2003).

<sup>b</sup>References: (1) Lundgren, Zepka, & Cordes (1995); (2) Nice, Splaver, & Stairs (2004) (3) Edwards, & Bailes (2001) ; (4) Kaspi et al. (2000) ; (5) Bailes et al. (2003).



Table 2. Estimates for the Galactic coalescence rate ( $\mathcal{R}_{\text{tot}}$ ) of NS–WD binaries at various confidence limits for all models considered.

Model <sup>a</sup>	$\mathcal{R}_{\text{tot}}$ (Myr <sup>-1</sup> )		
	peak <sup>b</sup>	68% <sup>c</sup>	95% <sup>c</sup>
1	1.23	+1.57 -0.77	+3.97 -1.04
2	1.00	+1.27 -0.62	+3.20 -0.83
3	1.32	+1.69 -0.83	+4.27 -1.12
4	1.53	+1.99 -0.97	+5.02 -1.31
5	1.19	+1.53 -0.75	+3.87 -1.01
<b>6</b>	4.11	+5.25 -2.56	+13.23 -3.47
7	1.73	+2.21 -1.08	+5.57 -1.46
8	0.83	+1.07 -0.52	+2.71 -0.71
9	0.43	+0.55 -0.27	+1.39 -0.36
10	1.42	+1.88 -0.92	+4.76 -1.23
11	0.72	+0.96 -0.47	+2.42 -0.62
12	0.55	+0.72 -0.35	+1.82 -0.47
13	0.40	+0.53 -0.26	+1.33 -0.34
14	0.23	+0.30 -0.15	+0.76 -0.20
15	10.03	+12.46 -6.09	+31.38 -8.34
16	3.68	+4.57 -2.25	+11.53 -3.07
17	2.45	+3.06 -1.50	+7.71 -2.04
18	1.55	+1.94 -0.95	+4.90 -1.29
19	0.72	+0.91 -0.44	+2.29 -0.60
20	5.48	+6.69 -3.29	+16.86 -4.52
21	1.96	+2.37 -1.17	+5.96 -1.61
22	1.55	+1.97 -0.96	+4.96 -1.3
23	1.13	+1.47 -0.71	+3.72 -0.97
24	1.14	+1.49 -0.73	+3.76 -0.98
25	1.21	+1.56 -0.76	+3.95 -1.03
26	1.33	+1.72 -0.84	+4.35 -1.13
27	1.46	+1.90 -0.93	+4.79 -1.25

<sup>a</sup>Model No. (see paper I for details of model parameters.)

<sup>b</sup>Peak value of the probability density function.

<sup>c</sup>Confidence limits.

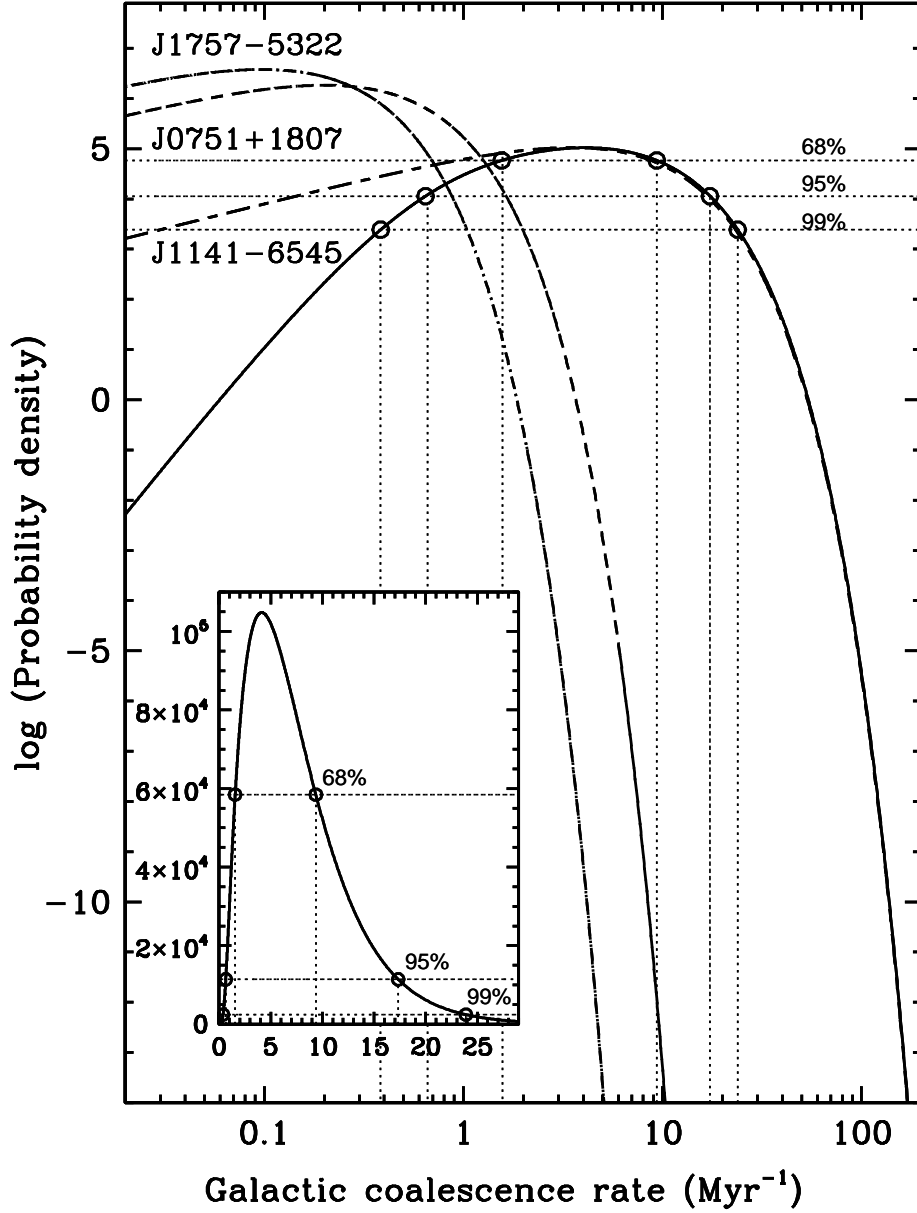


Fig. 1.— The PDFs of the Galactic coalescence rate estimation in both a logarithmic and a linear scale (inset) are shown for the reference model. The solid line represents  $P(\mathcal{R}_{\text{tot}})$ . Other curves are  $P(\mathcal{R})$  for PSRs J1757–5322 (dot-dash), J0751+1807 (short-dash), and J1141–6545 (long-and-short dash)-like populations, respectively. Dotted lines correspond to 68%, 95%, and 99% confidence limits for  $P(\mathcal{R}_{\text{tot}})$ .

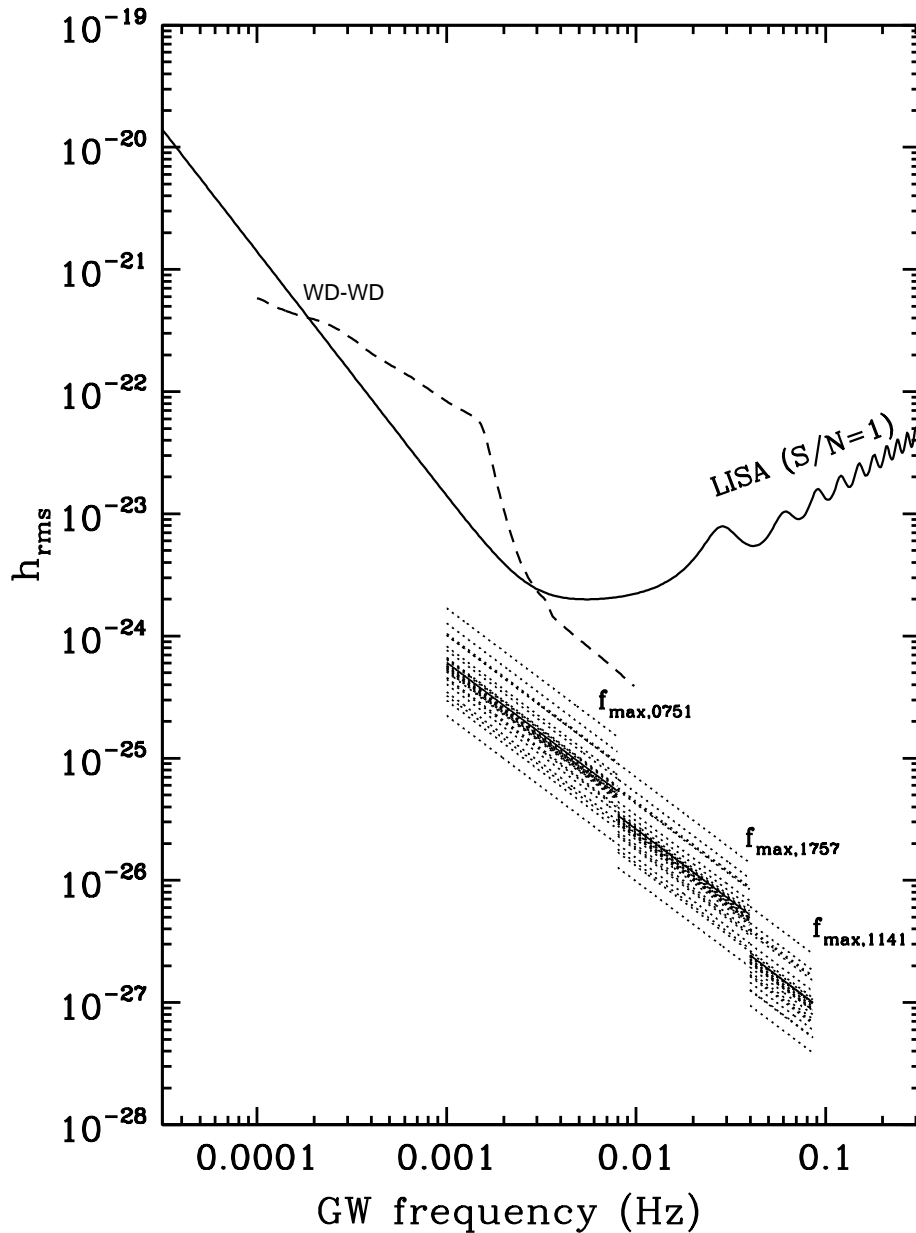


Fig. 2.— The effective GW amplitude  $h_{\text{rms}}$  for coalescing NS–WD binaries overlapped with the LISA sensitivity curve. The curve is produced with the assumption of  $S/N=1$  for 1 yr of integration. Dotted lines are results from all models we consider except the reference model, which is shown as a solid line. We also show the expected confusion noise from Galactic WD–WD binaries for comparison (dashed line).